Supplemental Material can be found at:
http://dmd.aspetjournals.org/content/suppl/2010/09/16/dmd.110.034140.DC1.html

0090-9556/10/3812-2100–2104$20.00
DRUG METABOLISM AND DISPOSITION
Copyright © 2010 by The American Society for Pharmacology and Experimental Therapeutics
DMD 38:2100–2104, 2010

Vol. 38, No. 12
34140/3644838
Printed in U.S.A.

DMD

DRUG METABOLISM AND DISPOSITION

aspet

Short Communication

*CYP3A4*16* and *CYP3A4*18* Alleles Found in East Asians Exhibit Differential Catalytic Activities for Seven CYP3A4 Substrate Drugs[S]

Received April 28, 2010; accepted September 16, 2010

ABSTRACT:

CYP3A4, the major form of cytochrome P450 (P450) expressed in the adult human liver, is involved in the metabolism of approximately 50% of commonly prescribed drugs. Several genetic polymorphisms in *CYP3A4* are known to affect its catalytic activity and to contribute in part to interindividual differences in the pharmacokinetics and pharmacodynamics of CYP3A4 substrate drugs. In this study, catalytic activities of the two alleles found in East Asians, *CYP3A4*16* (T185S) and *CYP3A4*18* (L293P), were assessed using the following seven substrates: midazolam, carbamazepine, atorvastatin, paclitaxel, docetaxel, irinotecan, and terfenadine. The holoprotein levels of CYP3A4.16 and CYP3A4.18 were significantly higher and lower, respectively, than that of CYP3A4.1 when expressed in Sf21 insect cell microsomes together with human NADPH-P450 reductase. CYP3A4.16 exhibited intrinsic clearances (V_{max}/K_m) that were lowered considerably (by 84–60%) for metabolism of midazolam, carbamazepine, atorvastatin, paclitaxel, and irinotecan compared with CYP3A4.1 due to increased K_m with or without decreased V_{max} values, whereas no apparent decrease in intrinsic clearance was observed for docetaxel. On the other hand, K_m values for CYP3A4.18 were comparable to those for CYP3A4.1 for all substrates except terfenadine; but V_{max} values were lower for midazolam, paclitaxel, docetaxel, and irinotecan, resulting in partially reduced intrinsic clearance values (by 34–52%). These results demonstrated that the impacts of both alleles on CYP3A4 catalytic activities depend on the substrates used. Thus, to evaluate the influences of both alleles on the pharmacokinetics of CYP3A4-metabolized drugs and their drug-drug interactions, substrate drug-dependent characteristics should be considered for each drug.

Introduction

CYP3A4, the major form of cytochrome P450 (P450) expressed in the adult human liver, is involved in the metabolism of approximately 50% of commonly prescribed drugs (Guengerich, 1999). CYP3A4 is capable of oxidizing a wide range of structurally diverse drugs as well as endogenous compounds. For example, many anticancer drugs, such as docetaxel, paclitaxel, etoposide, tamoxifen, irinotecan, vinblastine, and cyclophosphamide, are known to be metabolized by CYP3A4.

The expression and catalytic activity of CYP3A are highly variable among individuals, and this variability is partially attributable to genetic factors (Ozdemir et al., 2000). Several *CYP3A4* genetic polymorphisms are known to affect the metabolism of CYP3A4 substrate drugs (www.cypalleles.ki.se/cyp3a4.htm). In addition, *CYP3A4* alleles were reported to exhibit large ethnic differences in their distribution. In the Japanese, four alleles with amino acid alterations, *CYP3A4*6* (D277EfsX8), *CYP3A4*11* (T363M), *CYP3A4*16* (T185S), and *CYP3A4*18* (L293P), are found at frequencies of <0.001, 0.002, 0.014 to 0.05, and 0.013 to 0.028, respectively (Lamba et al., 2002; Yamamoto et al., 2003; Fukushima-Uesaka et al., 2004). Of these alleles, *CYP3A4*16* has also been detected in Korean (allele frequency, 0.002) and Mexican populations (allele frequency, 0.05) and *CYP3A4*18* is distributed commonly among East Asians such as Chinese (allele frequency, 0.008–0.01), Koreans (allele frequency, 0.012–0.017), and Malaysians (allele frequency, 0.021) (Wen et al., 2004; Hu et al., 2005; Lee et al., 2007; Ruzilawati et al., 2007; Kang et al., 2009).

*CYP3A4*16* and *CYP3A4*18* are reported to affect both in vitro and in vivo catalytic activities toward several substrates and to be involved in the interindividual differences in the pharmacokinetics and pharmacodynamics of CYP3A4 substrate drugs. CYP3A4.16 exhibited an approximately 50% reduction in intrinsic clearance (V_{max}/K_m) for testosterone (TST) 6β-hydroxylation activity in vitro (Murayama et al., 2002). We recently demonstrated the substrate-dependent altered kinetics of CYP3A4.16 for midazolam (MDZ) and carbamazepine (CBZ) (Maekawa et al., 2009). The intrinsic clearance for 1′-hydroxymidazolam (1′-OH-MDZ), 4-hydroxymidazolam (4-

This study was supported in part by the Program for the Promotion of Fundamental Studies in Health Sciences; and the Health and Labor Sciences Research Grants from the Ministry of Health, Labor and Welfare.

K.M., N.H., and T.Y. contributed equally to this work.

Article, publication date, and citation information can be found at http://dmd.aspetjournals.org.

doi:10.1124/dmd.110.034140.

[S] The online version of this article (available at http://dmd.aspetjournals.org) contains supplemental material.

ABBREVIATIONS: P450, cytochrome P450; APC, 7-ethyl-10-[4-*N*-(5-aminopentanoic acid)-1-piperidino] carbonyloxycamptothecin; TST, testosterone; MDZ, midazolam; CBZ, carbamazepine; 1′-OH-MDZ, 1′-hydroxymidazolam; ATV, atorvastatin; PTX, paclitaxel; DTX, docetaxel; IRN, irinotecan; TFN, terfenadine; 4-OH-MDZ, 4-hydroxymidazolam; 3′-*p*-OH-PTX, 3′-*p*-hydroxypaclitaxel; 2-OH-ATV, 2-hydroxyatorvastatin; 4-OH-ATV, 4-hydroxyatorvastatin; NPC, 7-ethyl-10-(4-amino-1-piperidino) carbonyloxycamptothecin; OR, NADPH P450 reductase.

OH-MDZ), and CBZ 10,11-epoxide formation decreased by 50, 30, and 74%, respectively, compared with the wild type. In vivo, heterozygous *CYP3A4*16* patients administered paclitaxel (PTX) showed significantly reduced 3′-*p*-hydroxypaclitaxel (3′-*p*-OH-PTX)/PTX area under the plasma concentration-time curve ratios (Nakajima et al., 2006). In addition, decreased metabolism of irinotecan (IRN) to the inactive metabolite 7-ethyl-10-[4-*N*-(5-aminopentanoic acid)-1-piperidino] carbonyloxycamptothecin (APC) was observed with *CYP3A4*16* (Sai et al., 2008).

In contrast to *CYP3A4*16*, *CYP3A4*18* seems to be bidirectional in terms of its catalytic activity toward different substrates, although different evaluation systems were used for each study. For example, the CYP3A4.18 protein exhibited increased activity for TST and chlorpyrifos (Dai et al., 2001), but not for nifedipine (Lee et al., 2005) in vitro. On the other hand, for the conventional probe drug MDZ, CYP3A4.18 showed decreased metabolism in vitro but not in vivo (Lee et al., 2007). Kang et al. (2009) demonstrated that *CYP3A4*18* is the gain-of-function allele for metabolism of several CYP3A4 substrates, including sex steroids like estrogens, leading to a relative sex-hormone deficiency that may predispose older women to osteoporosis.

In this study, to evaluate the effects of *CYP3A4*16* and *CYP3A4*18* on the catalytic activity toward structurally diverse substrates, recombinant wild-type (CYP3A4.1) and variant CYP3A4 enzymes (CYP3A4.16 and CYP3A4.18) were expressed using baculovirus-insect cell systems. The seven substrates used in the investigation were MDZ, CBZ, atorvastatin (ATV), PTX, docetaxel (DTX), IRN, and terfenadine (TFN) (Supplemental Fig. S1).

Materials and Methods

Materials. Purified human cytochrome b_5 was purchased from either Invitrogen (Carlsbad, CA) or Oxford Biomedical Research (Rochester, MI). MDZ and PTX were obtained from Wako Pure Chemicals (Osaka, Japan). 1′-OH-MDZ and 4-OH-MDZ were obtained from BD Gentest (Woburn, MA). CBZ, CBZ 10,11-epoxide, 3′-*p*-OH-PTX, and TFN and its metabolite *t*-butylhydroxyterfenadine were purchased from Sigma-Aldrich (St. Louis, MO). A second TFN metabolite, α,α-diphenyl-4-piperidinomethanol, was obtained from Fine & Performance Chemicals Ltd (Middlesbrough, UK). ATV, its metabolites 2-hydroxyatorvastatin (2-OH-ATV) and 4-hydroxyatorvastatin (4-OH-ATV), and DTX and its metabolite, DTX hydroxy *tert*-butyl carbamate (M2), were obtained from Toronto Research Chemicals Inc. (North York, ON, Canada). IRN and its CYP3A4 metabolites, APC, and 7-ethyl-10-(4-amino-1-piperidino) carbonyloxycamptothecin (NPC), were kindly supplied by Yakult (Tokyo, Japan). All other chemicals and solvents used were of the highest commercially available grade or analytical grade.

Expression of Recombinant Wild-Type and Mutant CYP3A4 Proteins. Insect cell microsomes coexpressing CYP3A4 (wild type or variants) and NADPH P450 reductase (OR) were prepared according to methods described previously (Maekawa et al., 2009). The cytochrome P450 content and OR activity in microsomes were measured (Phillips and Langdon, 1962; Omura and Sato, 1964), and Western blotting of CYP3A4 and OR was performed as described previously (Maekawa et al., 2009).

Assay for CYP3A4 Activity. To compare alterations in kinetic parameters among substrates, three batches of wild-type and two variant enzyme preparations were used for all kinetic studies. Kinetic analysis on all seven CYP3A4 substrates was performed under proper conditions for the incubation time and P450 concentrations such that linear relationships for metabolite formation were obtained.

Catalytic activities for MDZ 1′- and 4-hydroxylations and CBZ 10,11-epoxide formation were measured as described previously (Maekawa et al., 2009), with slight modifications. For other substrates (ATV, PTX, DTX, IRN, and TFN), the incubation conditions were similar to those used for MDZ and CBZ. For all substrates, CYP3A4s from insect microsomes and purified cytochrome b_5 were mixed together (CYP3A4/b_5 ratio, 1:4), and protein concentrations and the OR/P450 ratio in the CYP3A4 wild-type and variant reaction mixtures were adjusted to be equivalent by adding both control (uninfected) microsomes and microsomes expressing solely OR. MDZ (0.2–200 μM), CBZ (10–500 μM), ATV (5–120 μM), PTX (1–50 μM), DTX (0.25–64 μM), IRN (5–400 μM), or TFN (0.0125–160 μM) was added into aliquots of the above-mentioned enzyme preparations. The reaction was started by adding NADPH generation system and terminated by adding appropriate stop solutions containing suitable internal standard for the measurement of each metabolite. Samples were mixed well and then spun at 13,000*g* for 3 to 5 min.

Metabolite analyses for MDZ, CBZ, ATV, and PTX were carried out on a tandem quadrupole mass spectrometer (Micromass Quattro Premier XE; Waters, Milford, MA) interfaced with an Acquity UPLC System (Waters) equipped with an Acquity BEH C18 column (1.7 μm, 2.1 × 30 mm; Waters) kept at 50°C. Two solutions (solution A, 10 mM ammonium acetate; solution B, 90% acetonitrile containing 10 mM ammonium acetate) were used as the mobile phase. Metabolites were eluted by linear gradient, increasing solution B. Detections were performed by monitoring the transitions of *m/z* 342 to 203 (1′-OH-MDZ), *m/z* 342 to 234 (4-OH-MDZ), *m/z* 253 to 180 (CBZ 10,11-epoxide), *m/z* 575 to 440 (2-OH-ATV and 4-OH-ATV), and *m/z* 870 to 122 (3′-*p*-OH-PTX).

For IRN, TFN, and DTX, a time-of-flight mass spectrometer (Micromass LCT Premier XE; Waters) interfaced with an Acquity UPLC System, equipped with Acquity BEH C18 column (1.7 μm, 2.1 × 100 mm; Waters), and kept at 40°C was used for metabolite analyses. The mobile phase consisted of a mixture of acetonitrile/methanol/distilled water containing 0.1% (v/v) formic acid (14:14:72 for IRN, 21:21:58 for TFN, and 15:45:40 for DTX) delivered isocratically at a flow rate of 0.3 ml/min. Detections were performed by monitoring the M+H$^+$ ions, *m/z* 824.3493 ± 0.02 (*t*-butyl hydroxyl DTX), 519.2243 ± 0.02 (NPC), 619.2768 ± 0.02 (APC), 488.3165 ± 0.02 (*t*-butyl hydroxyl TFN), and 268.1701 ± 0.02 (α-α-diphenyl-4-piperidinomethanol).

Kinetic parameters were calculated using the computer program designed for nonlinear regression analysis (MULTI program) (Yamaoka et al., 1986). Kinetic parameters for MDZ 4-hydroxylation, ATV 2- and 4-hydroxylation, PTX 3′-*p*-hydroxylation, IRN oxidation to NPC, and DTX *t*-butyl hydroxylation were determined by the hyperbolic Michaelis-Menten model (eq. 1). The substrate inhibition model (eq. 2) was used for MDZ 1′-hydroxylation, TFN *C*-hydroxylation, and TFN *N*-demethylation, where K_s is the substrate inhibition constant. In the case of the 10,11-epoxidation of CBZ, kinetic parameters were determined by the modified two-site equation ($V_{max1} = 0$) (Korzekwa et al., 1998) (eq. 3).

$$V = V_{max}S/(K_m + S) \quad (1)$$

$$V = V_{max}S/(K_m + S + S^2/K_s) \quad (2)$$

$$V = (V_{max2}S^2/K_{m1}K_{m2})/(1 + S/K_{m1} + S^2/K_{m1}K_{m2}) \quad (3)$$

Kinetic data were determined as the mean ± S.D. for three microsomal preparations derived from separate baculovirus infections, and statistical analysis was conducted by Dunnett's multiple comparison test in SAS (SAS Institute, Cary, NC). A p value of <0.05 was set as a statistically significant difference.

Results and Discussion

Expression of Wild-Type and Variant CYP3A4s in Insect Cells. Wild-type (CYP3A4.1) and variant proteins (CYP3A4.16 and CYP3A4.18) were coexpressed with human OR in Sf21 insect cells. Typical CO difference spectra with a maximum absorbance at 450 nm were obtained for all microsomal fraction preparations (Supplemental Fig. S2). CYP3A4.18 exhibited a larger peak at 420 nm than either CYP3A4.1 or CYP3A4.16. In three independent expression experiments, holoenzyme contents in the variant CYP3A4.16 (230.8 ± 25.2 pmol/mg microsomal protein) and CYP3A4.18 microsomes (51.3 ± 3.2 pmol/mg microsomal protein) were significantly higher and lower ($p < 0.05$), respectively, than that in the wild-type

DMD DRUG METABOLISM AND DISPOSITION aspet

TABLE 1

Kinetic parameters for 10 catalytic reactions using seven substrates by CYP3A4.1, CYP3A4.16, and CYP3A4.18

Data are represented by mean ± S.D. of three different expression experiments.

	K_m	V_{max}	Intrinsic Clearance (V_{max}/K_m)	K_s
	μM	*pmol/min/pmol P450*	*μl/min/pmol P450*	*μM*
MDZ 1'-hydroxylation				
CYP3A4.1	1.9 ± 0.1	28.1 ± 2.8	14.8 ± 1.5	407 ± 32
CYP3A4.16	2.6 ± 0.1***	15.0 ± 3.5**	5.8 ± 1.7***	986 ± 302*
CYP3A4.18	2.0 ± 0.1	17.5 ± 3.2*	8.8 ± 1.6**	713 ± 168
MDZ 4-hydroxylation				
CYP3A4.1	23.1 ± 5.2	12.9 ± 0.1	0.58 ± 0.14	
CYP3A4.16	51.5 ± 3.5***	11.7 ± 1.4	0.23 ± 0.04*	
CYP3A4.18	22.3 ± 3.5	9.2 ± 2.0*	0.42 ± 0.11	
CBZ epoxidation[a]				
CYP3A4.1	21.9 ± 5.2 (K_{m1}) 165 ± 15 (K_{m2})	15.5 ± 2.5	0.095 ± 0.018	
CYP3A4.16	48.0 ± 3.7***(K_{m1}) 603 ± 204** (K_{m2})	11.0 ± 1.0	0.020 ± 0.008***	
CYP3A4.18	20.0 ± 2.7 (K_{m1}) 172 ± 32 (K_{m2})	15.7 ± 4.5	0.090 ± 0.011	
ATV 2-hydroxylation				
CYP3A4.1	24.2 ± 7.6	6.6 ± 1.1	0.29 ± 0.08	
CYP3A4.16	87.4 ± 22.6**	8.2 ± 1.9	0.10 ± 0.02*	
CYP3A4.18	20.2 ± 6.8	3.8 ± 1.3	0.20 ± 0.11	
ATV 4-hydroxylation				
CYP3A4.1	19.6 ± 4.0	16.1 ± 5.0	0.84 ± 0.29	
CYP3A4.16	65.4 ± 19.3**	8.4 ± 1.4	0.14 ± 0.05*	
CYP3A4.18	16.1 ± 3.4	11.1 ± 4.2	0.71 ± 0.31	
PTX 3'-*p*-hydroxylation				
CYP3A4.1	2.9 ± 0.1	0.55 ± 0.06	0.19 ± 0.03	
CYP3A4.16	12.9 ± 2.4***	0.55 ± 0.13	0.04 ± 0.02***	
CYP3A4.18	2.7 ± 0.1	0.24 ± 0.07**	0.09 ± 0.03**	
DTX *t*-butyl hydroxylation				
CYP3A4.1	2.5 ± 0.1	0.38 ± 0.01	0.16 ± 0.01	
CYP3A4.16	1.8 ± 0.2**	0.26 ± 0.03**	0.14 ± 0.01	
CYP3A4.18	2.3 ± 0.2	0.24 ± 0.04**	0.10 ± 0.03*	
IRN oxidation to NPC				
CYP3A4.1	19.3 ± 2.7	1.4 ± 0.2	0.07 ± 0.02	
CYP3A4.16	34.0 ± 2.9**	0.9 ± 0.4	0.03 ± 0.01*	
CYP3A4.18	19.7 ± 2.8	0.7 ± 0.1*	0.04 ± 0.01*	
TFN *t*-butyl hydroxylation				
CYP3A4.1	3.4 ± 0.3	3.4 ± 0.6	1.0 ± 0.2	218 ± 5
CYP3A4.16	3.5 ± 0.5	2.1 ± 0.1*	0.6 ± 0.1*	51 ± 8
CYP3A4.18	6.0 ± 1.2*	3.1 ± 0.5	0.5 ± 0.1*	311 ± 131
TFN *N*-demethylation[b]				
CYP3A4.1	2.4 ± 0.5	2.2 ± 0.4	0.95 ± 0.25	629 ± 244
CYP3A4.16	2.1 ± 0.2	1.5 ± 0.3	0.72 ± 0.12	92 ± 8
CYP3A4.18	3.4 ± 0.3*	1.9 ± 0.2	0.57 ± 0.10	

* $p < 0.05$, ** $p < 0.01$, and *** $p < 0.001$ versus the wild-type (Dunnett's multiple comparison test).

[a] For CBZ epoxidation, K_{m1} and K_{m2}, V_{max2}, and intrinsic clearance (V_{max2}/K_{m2}) values are indicated in each column.

[b] For TFN *N*-demethylation, kinetic profile of CYP3A4.18 was better fitted to the Michaelis-Menten model than to the substrate inhibition model.

CYP3A4.1 microsomes (104.4 ± 23.9 pmol/mg microsomal protein). OR activity varied among the preparations but was not significantly different ($p > 0.05$) among CYP3A4.1 (1032.3 ± 88.2 nmol cytochrome *c* reduced/min/mg protein), CYP3A4.16 (659.4 ± 254.6 cytochrome *c* reduced/min/mg protein), and CYP3A4.18 (1019.1 ± 260.1 cytochrome *c* reduced/min/mg protein). On the other hand, total (apoenzyme and holoenzyme) CYP3A4 protein expression levels in insect cell microsomes were not significantly different ($p > 0.05$) between the wild type and variants by immunoblot analysis (data not shown).

Catalytic Activities of Wild-Type and Variant CYP3A4s. To characterize the substrate-dependent functional alterations of *CYP3A4*16* and *CYP3A4*18*, CYP3A4 catalytic activities of wild type and variants toward the seven substrates (MDZ, CBZ, ATV, PTX, DTX, IRN, and TFN) were measured. For four of the substrates, two different metabolites were detected: 1'- and 4-OH-MDZ from MDZ, 2- and 4-OH-ATV from ATV, APC and NPC from IRN, and *t*-butylhydroxy-TFN and α-α diphenyl-4-piperidinomethanol (azacyclonol) from TFN. Because the level of APC formed from IRN was too low to quantify precisely under our experimental conditions, kinetic analysis for IRN was performed only for NPC formation. The kinetic profiles are shown in Supplemental Fig. S3, and kinetic parameters are summarized in Table 1. The variant-to-wild-type ratios (percent) of intrinsic clearance values (V_{max}/K_m) are compared among substrates used (Fig. 1).

CYP3A4.16 showed significantly higher K_m values than CYP3A4.1 for seven catalytic reactions: MDZ 1'- and 4-hydroxylations ($p < 0.001$), CBZ 10,11-epoxidation ($p < 0.01$), ATV 2- and 4-hydroxylations ($p < 0.01$), PTX 3'-*p*-hydroxylation ($p < 0.001$), and IRN oxidation to NPC ($p < 0.01$). The V_{max} value of CYP3A4.16 was significantly lower (by 47%) ($p < 0.01$) for MDZ 1'-hydroxylation, but not for MDZ 4-hydroxylation (91% of the wild type), suggesting that catalytic site-dependent changes in V_{max} values occurred. The intrinsic clearance (V_{max}/K_m) of CYP3A4.16 was significantly reduced compared to that of CYP3A4.1 for the following catalytic reactions: MDZ 1'- and 4-hydroxylations (by 61 and 60%,

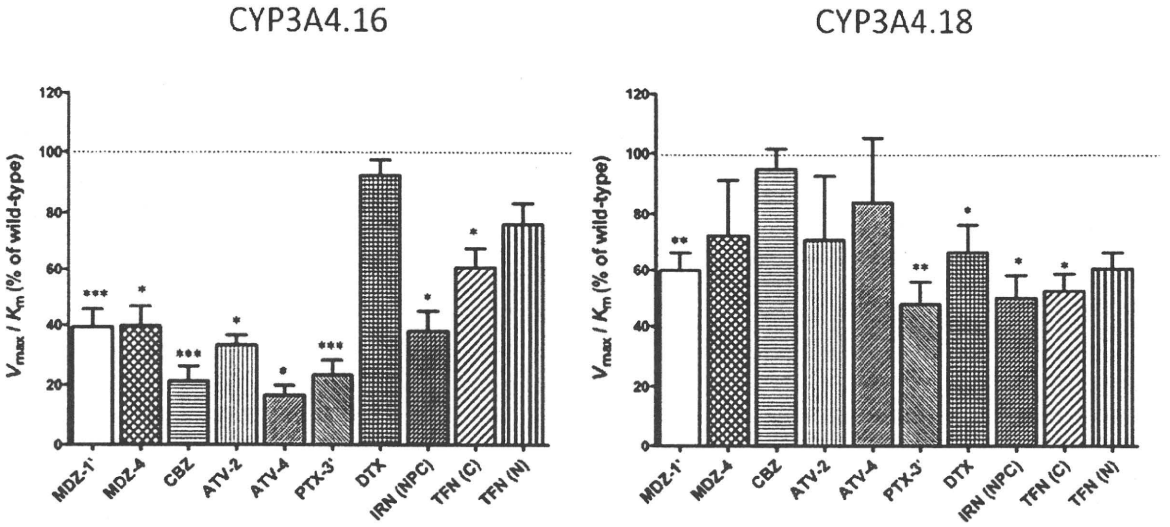

FIG. 1. The percent ratios of intrinsic clearance of variants to that of the wild type. Data are represented by mean ± S.D. of three different expression experiments. MDZ-1', MDZ 1'-hydroxylation; MDZ-4, MDZ 4-hydroxylation; CBZ, CBZ 10,11-epoxidation; ATV-2, ATV 2-hydroxylation; ATV-4, ATV 4-hydroxylation; PTX-3', PTX 3'-*p*-hydroxylation; DTX, DTX *t*-butyl hydroxylation; IRN (NPC), IRN oxidation to NPC; TFN (C), TFN *t*-butyl hydroxylation; TFN (N), TFN *N*-demethylation. * $p <$ 0.05, ** $p < 0.01$, and *** $p < 0.001$ versus the wild-type (Dunnett's multiple comparison test).

$p < 0.001$ and $p < 0.05$, respectively), CBZ 10,11-epoxidation (by 79%, $p < 0.001$), ATV 2- and 4-hydroxylation (by 67 and 84%, respectively, $p < 0.05$), PTX 3'-*p*-hydroxylation (by 77%, $p <$ 0.001), IRN oxidation to NPC (by 62%, $p < 0.05$), and TFN *t*-butyl hydroxylation (by 40%, $p < 0.05$). In contrast, for DTX hydroxylation and TFN *N*-demethylation, no significant differences ($p > 0.05$) in the intrinsic clearance values were observed between CYP3A4.1 and CYP3A4.16.

Our results were consistent with those by Miyazaki et al. (2008), who found that recombinant CYP3A4.16 expressed in *Escherichia coli* is markedly deficient in MDZ, TST, and nifedipine metabolisms with lower V_{max} and increased K_m relative to CYP3A4.1. Thr185 in the E helix is far away from the active site and is not located in the substrate recognition site. Further studies are necessary to elucidate the role of this residue in the binding of structurally diverse CYP3A4 substrates to the substrate recognition site.

In agreement with the lower in vitro catalytic activity of CYP3A4.16 toward PTX and IRN, *CYP3A4*16* heterozygous patients administered PTX or IRN were reported to show significantly reduced metabolite-to-substrate area under the plasma concentration-time curve ratios, which are parameters for in vivo CYP3A4 activity (Nakajima et al., 2006; Sai et al., 2008). As for substrates for which the clinical significance of *CYP3A4*16* has not been evaluated, this study demonstrated that ATV metabolism was markedly affected by CYP3A4.16. Because CYP3A4 (but not CYP3A5) is the major enzyme involved in the formation of the two ATV metabolites: 2- and 4-OH-ATV (Park et al., 2008), the clinical relevance of *CYP3A4*16* for efficacy and/or adverse reactions of ATV should be further investigated. In contrast, CYP3A4.16 retained its catalytic activity toward DTX, and thus it is predicted that this allele does not substantially influence the metabolism of DTX in vivo.

For CYP3A4.18, the reduced intrinsic clearances were observed for MDZ 1'-hydroxylation (by 40%, $p < 0.01$), PTX 3'-*p*-hydroxylation (by 52%, $p < 0.01$), DTX *t*-butyl hydroxylation (by 32%, $p < 0.05$), IRN oxidation to NPC (by 50%, $p < 0.05$), and TFN *t*-butyl hydroxylation (by 48%, $p < 0.05$) compared with CYP3A4.1. Except for TFN, the lowered V_{max} values for CYP3A4.18 resulted in lower activity in contrast to those for CYP3A4.16, which exhibited increased K_m values for most substrates. On the other hand, CYP3A4.18 had similar kinetic profiles to CYP3A4.1 in their values for K_m, V_{max}, and intrinsic clearance for oxidation of CBZ (Table 1; Supplemental Fig. S3), which has the lowest molecular weight among the seven substrates (Supplemental Fig. S1).

For the substrates MDZ, PTX, and IRN, it was reported that heterozygous *CYP3A4*1/CYP3A4*18* did not affect their pharmacokinetics (Nakajima et al., 2006; Lee et al., 2007; Sai et al., 2008). Because our in vitro results with CYP3A4.18 showed a partial decrease in V_{max} values for these drugs, an in vivo-in vitro correlation was not observed, at least for heterozygotes. Further studies are necessary to evaluate the clinical relevance of homozygous *CYP3A4*18*.

By molecular modeling studies, Kang et al. (2009) demonstrated that the L293P substitution at the beginning of the I helix caused significant secondary structural changes in the I helix and reduced protein stability. Our spectral analysis that CYP3A4.18 preparations contained more P420 than CYP3A4.1 might also be in agreement with their modeling. These possible conformational changes in CYP3A4.18 may affect substrate access depending on the substrate structure.

In conclusion, the substrate-dependent functional alterations of CYP3A4.16 and CYP3A4.18 were assessed toward seven structurally diverse substrates, MDZ, CBZ, ATV, PTX, DTX, IRN, and TFN. Compared to the wild type, CYP3A4.16 exhibited more than 60% reduced activity toward MDZ, CBZ, ATV, PTX, and IRN due to increased K_m values. In contrast, CYP3A4.18 showed a moderate reduction in its catalytic activity (by 34–52%) for MDZ, PTX, DTX, and IRN due to decreased V_{max} values. Thus, to evaluate the influences of both alleles on the pharmacokinetics of other CYP3A4-metabolized drugs and their drug-drug interactions, substrate drug-dependent characteristics should be elucidated for each drug.

Acknowledgments. We thank Chie Sudo for secretarial assistance and Yakult Honsha Co. Ltd. for providing irinotecan and its CYP3A4 metabolites.

Project Team for Pharmacogenetics (K.M., N.H., S.-R.K., K.S., N.K., M.T., H.O., J.S., Y.S.), Division of Medicinal Safety Science (K.M., M.T., R.H., Y.S.), Division of Functional Biochemistry and Genomics (K.S., M.N., J.S.), Division of Drugs (N.K.), and Division of Organic Chemistry (H.O.), National Institute of Health Sciences, Tokyo, Japan; and DMPK Research Laboratory, Research Division, Mitsubishi Tanabe Pharma Corporation, Chiba, Japan (T.Y., Y.F., F.A., T.N.)

KEIKO MAEKAWA
NORIKO HARAKAWA
TAKUYA YOSHIMURA
SU-RYANG KIM
YOSHIYUKI FUJIMURA
FUMIKA AOHARA
KIMIE SAI
NORIKO KATORI
MASAHIRO TOHKIN
MIKIHIKO NAITO
RYUICHI HASEGAWA
HARUHIRO OKUDA
JUN-ICHI SAWADA[1]
TAKURO NIWA
YOSHIRO SAITO

[1] Current affiliation: Office of Biologics I, Pharmaceuticals and Medical Devices Agency, Chiyoda-ku, Tokyo, Japan.

References

Dai D, Tang J, Rose R, Hodgson E, Bienstock RJ, Mohrenweiser HW, and Goldstein JA (2001) Identification of variants of CYP3A4 and characterization of their abilities to metabolize testosterone and chlorpyrifos. *J Pharmacol Exp Ther* **299:**825–831.

Fukushima-Uesaka H, Saito Y, Watanabe H, Shiseki K, Saeki M, Nakamura T, Kurose K, Sai K, Komamura K, Ueno K, et al. (2004) Haplotypes of CYP3A4 and their close linkage with CYP3A5 haplotypes in a Japanese population. *Hum Mutat* **23:**100.

Guengerich FP (1999) Cytochrome P-450 3A4: regulation and role in drug metabolism. *Annu Rev Pharmacol Toxicol* **39:**1–17.

Hu YF, He J, Chen GL, Wang D, Liu ZQ, Zhang C, Duan LF, and Zhou HH (2005) CYP3A5*3 and CYP3A4*18 single nucleotide polymorphisms in a Chinese population. *Clin Chim Acta* **353:**187–192.

Kang YS, Park SY, Yim CH, Kwak HS, Gajendrarao P, Krishnamoorthy N, Yun SC, Lee KW, and Han KO (2009) The CYP3A4*18 genotype in the cytochrome P450 3A4 gene, a rapid metabolizer of sex steroids, is associated with low bone mineral density. *Clin Pharmacol Ther* **85:**312–318.

Korzekwa KR, Krishnamachary N, Shou M, Ogai A, Parise RA, Rettie AE, Gonzalez FJ, and Tracy TS (1998) Evaluation of atypical cytochrome P450 kinetics with two-substrate models: evidence that multiple substrates can simultaneously bind to cytochrome P450 active sites. *Biochemistry* **37:**4137–4147.

Lamba JK, Lin YS, Thummel K, Daly A, Watkins PB, Strom S, Zhang J, and Schuetz EG (2002) Common allelic variants of cytochrome P4503A4 and their prevalence in different populations. *Pharmacogenetics* **12:**121–132.

Lee SJ, Bell DA, Coulter SJ, Ghanayem B, and Goldstein JA (2005) Recombinant CYP3A4*17 is defective in metabolizing the hypertensive drug nifedipine, and the CYP3A4*17 allele may occur on the same chromosome as CYP3A5*3, representing a new putative defective CYP3A haplotype. *J Pharmacol Exp Ther* **313:**302–309.

Lee SJ, Lee SS, Jeong HE, Shon JH, Ryu JY, Sunwoo YE, Liu KH, Kang W, Park YJ, Shin CM, et al. (2007) The CYP3A4*18 allele, the most frequent coding variant in asian populations, does not significantly affect the midazolam disposition in heterozygous individuals. *Drug Metab Dispos* **35:**2095–2101.

Maekawa K, Yoshimura T, Saito Y, Fujimura Y, Aohara F, Emoto C, Iwasaki K, Hanioka N, Narimatsu S, Niwa T, et al. (2009) Functional characterization of CYP3A4.16: catalytic activities toward midazolam and carbamazepine. *Xenobiotica* **39:**140–147.

Miyazaki M, Nakamura K, Fujita Y, Guengerich FP, Horiuchi R, and Yamamoto K (2008) Defective activity of recombinant cytochromes P450 3A4.2 and 3A4.16 in oxidation of midazolam, nifedipine, and testosterone. *Drug Metab Dispos* **36:**2287–2291.

Murayama N, Nakamura T, Saeki M, Soyama A, Saito Y, Sai K, Ishida S, Nakajima O, Itoda M, Ohno Y, et al. (2002) CYP3A4 gene polymorphisms influence testosterone 6beta-hydroxylation. *Drug Metab Pharmacokinet* **17:**150–156.

Nakajima Y, Yoshitani T, Fukushima-Uesaka H, Saito Y, Kaniwa N, Kurose K, Ozawa S, Aoyagi N, Kamatani N, Yamamoto N, et al. (2006) Impact of the haplotype CYP3A4*16B harboring the Thr185Ser substitution on paclitaxel metabolism in Japanese patients with cancer. *Clin Pharmacol Ther* **80:**179–191.

Omura T and Sato R (1964) The carbon monoxide-binding pigment of liver microsomes. I. Evidence for its hemoprotein nature. *J Biol Chem* **239:**2370–2378.

Ozdemir V, Kalow W, Tang BK, Paterson AD, Walker SE, Endrenyi L, and Kashuba AD (2000) Evaluation of the genetic component of variability in CYP3A4 activity: a repeated drug administration method. *Pharmacogenetics* **10:**373–388.

Park JE, Kim KB, Bae SK, Moon BS, Liu KH, and Shin JG (2008) Contribution of cytochrome P450 3A4 and 3A5 to the metabolism of atorvastatin. *Xenobiotica* **38:**1240–1251.

Phillips AH and LANGDON RG (1962) Hepatic triphosphopyridine nucleotide-cytochrome c reductase: isolation, characterization, and kinetic studies. *J Biol Chem* **237:**2652–2660.

Ruzilawati AB, Suhaimi AW, and Gan SH (2007) Genetic polymorphisms of CYP3A4: CYP3A4*18 allele is found in five healthy Malaysian subjects. *Clin Chim Acta* **383:**158–162.

Sai K, Saito Y, Fukushima-Uesaka H, Kurose K, Kaniwa N, Kamatani N, Shirao K, Yamamoto N, Hamaguchi T, Kunitoh H, et al. (2008) Impact of CYP3A4 haplotypes on irinotecan pharmacokinetics in Japanese cancer patients. *Cancer Chemother Pharmacol* **62:**529–537.

Wen S, Wang H, Ding Y, Liang H, and Wang S (2004) Screening of 12 SNPs of CYP3A4 in a Chinese population using oligonucleotide microarray. *Genet Test* **8:**411–416.

Yamamoto T, Nagafuchi N, Ozeki T, Kubota T, Ishikawa H, Ogawa S, Yamada Y, Hirai H, and Iga T (2003) CYP3A4*18: it is not rare allele in Japanese population. *Drug Metab Pharmacokinet* **18:**267–268.

Yamaoka K, Tanaka H, Okumura K, Yasuhara M, and Hori R (1986) An analysis program MULTI(ELS) based on extended nonlinear least squares method for microcomputers. *J Pharmacobiodyn* **9:**161–173.

Address correspondence to: Dr. Keiko Maekawa, Division of Medicinal Safety Science, National Institute of Health Sciences, 1-18-1 Kamiyoga, Setagaya-ku, Tokyo 158-8501, Japan. E-mail: maekawa@nihs.go.jp

DMD DRUG METABOLISM AND DISPOSITION aspet

Epilepsia, 51(12):2461–2465, 2010
doi: 10.1111/j.1528-1167.2010.02766.x

BRIEF COMMUNICATION

*HLA-B*1511* is a risk factor for carbamazepine-induced Stevens-Johnson syndrome and toxic epidermal necrolysis in Japanese patients

***Nahoko Kaniwa, *Yoshiro Saito, †Michiko Aihara, ‡Kayoko Matsunaga, *Masahiro Tohkin, *Kouichi Kurose, §Hirokazu Furuya, ¶Yukitoshi Takahashi, #Masaaki Muramatsu, **Shigeru Kinoshita, ‡Masamichi Abe, ¶Hiroko Ikeda, #Mariko Kashiwagi, #Yixuan Song, **Mayumi Ueta, **Chie Sotozono, †Zenro Ikezawa, and *Ryuichi Hasegawa, for the JSAR research group[1]**

*Division of Medicinal Safety Sciences, National Institute of Health Sciences, Tokyo, Japan; †Department of Environmental Immunodermatology, Yokohama City University Graduate School of Medicine, Yokohama, Japan; ‡Department of Dermatology, Fujita Health University School of Medicine, Toyoake, Japan; §Department of Neurology, Neuro-Muscular Center, National Oomuta Hospital Oomuta, Japan; ¶Shizuoka Institute of Epilepsy and Neurological Disorders, National Epilepsy Center, Shizuoka, Japan; #Molecular Epidemiology, Medical Research Institute, Tokyo Medical and Dental University, Tokyo, Japan; and **Department of Ophthalmology, Kyoto Prefectural University of Medicine, Kyoto, Japan

Summary

Stevens-Johnson syndrome (SJS) and toxic epidermal necrolysis (TEN) are rare but life-threatening severe cutaneous adverse reactions. Recently, strong associations of *HLA-B*1502* with carbamazepine-induced SJS/TEN have been found in Han Chinese patients. These associations have been confirmed in several Asian populations, excluding Japanese. SJS patients carrying *HLA-B*1508*, *HLA-B*1511*, or *HLA-B*1521*, which are members of the HLA-B75 type along with *HLA-B*1502*, were detected in studies in India and Thailand. In the current study, we genotyped the *HLA-B* locus from 14 Japanese typical and atypical SJS/TEN patients in whom carbamazepine was considered to be involved in the onset of adverse reactions. Although there were no *HLA-B*1502* carriers, four patients had *HLA-B*1511*. Our data suggest that *HLA-B*1511*, a member of *HLA-B75*, is a risk factor for carbamazepine-induced SJS/TEN in Japanese.

KEY WORDS: HLA-B*1502, HLA-B75, Serotype.

Stevens-Johnson syndrome (SJS) and toxic epidermal necrolysis (TEN) are severe adverse drug reactions (ADRs) with mucosal and cutaneous disorders, and often are accompanied by high fever and systemic complications. Although incidence is low, SJS and TEN are life-threatening and their mortalities are estimated at 5% and 30%, respectively. On the basis of summarized spontaneous reports of severe ADRs to the Ministry of Health, Labor and Welfare (MHLW) from 2006 to 2008, the incidence of SJS/TEN in Japan can be calculated as 3.4 patients per million per year (approximately 430 cases annually), and major causative drugs are allopurinol and carbamazepine.

Accepted September 3, 2010; Early View publication November 3, 2010.

Address correspondence to Nahoko Kaniwa, PhD, Division of Medicinal Safety Sciences, National Institute of Health Sciences, 1-18-1 Kamiyoga, Setagaya-ku, Tokyo 158-8501, Japan. E-mail: nkaniwa@nihs.go.jp

[1]The JSAR (Japan Severe Adverse Reactions) research group: the representative of the research group is Nahoko Kaniwa at National Institute of Health Sciences, and all authors are members of the research group.

As for carbamazepine-induced SJS/TEN, involvement of *HLA-B*1502* in Han Chinese SJS/TEN patients has been reported (Chung et al., 2004), and has been confirmed in Asians in Hong Kong (Man et al., 2007), Europe (Lonjou et al., 2006), Thailand (Locharernkul et al., 2008), and India (Mehta et al., 2009). However, no association between *HLA-B*1502* and carbamazepine-related SJS/TEN was detected in our previous study with seven Japanese SJS/TEN patients (Kaniwa et al., 2008). Therefore, we extended the investigation to explore other biomarkers in Japanese SJS/TEN patients who were administered carbamazepine.

Methods

Patients

The ethics committee of each participating institute of the JSAR (Japan Severe Adverse Reactions) research group approved this study. Written informed consent was obtained from each patient. Fifteen unrelated Japanese patients who were prescribed carbamazepine before the onset of SJS/TEN were recruited from participating institutes or through

a nationwide blood sampling network in Japan operated by the National Institute of Health Sciences in cooperation with the MHLW and the Federation of Pharmaceutical Manufacturers' Association of Japan. Patient characteristics are summarized in Table 1. Seven patients were included in our previous report (Kaniwa et al., 2008), and two patients were in another study (Ikeda et al., 2009). Twelve patients were diagnosed as definite SJS or TEN and three patients were diagnosed as probable SJS due to atypical or mild symptoms by the JSAR research group experts. This diagnosis was based on criteria proposed by Bastuji-Garin et al. (1993) using a standardized case report form including medicinal records, disease progress, and involvement of systemic complications as well as treatment. Severity of ocular complication was scored as follows: 0, no involvement; 1, only hyperemia of bulbar and palpebral conjunctiva; 2, pseudomembrane formation; 3, defect of conjunctival or corneal epithelia.

HLA-B typing

High-resolution *HLA-B* typing was performed by a sequence-based method using SeCore B Locus Sequencing kit (Invitrogen Corp., Brown Deer, WI, U.S.A.) and an ABI 3730 DNA sequencer (Applied Biosystems, Foster City, CA, U.S.A.). Genomic DNA (250 ng) was used for PCR amplification and sequencing exons 2, 3, and 4. HLA-B haplotype was estimated with the Assign SBT software (version 3.2.7b; Conexio Genomics, Applecross, WA, Australia).

Statistical analysis

*HLA-B*1511* allele frequency reported by Tanaka et al. was used as the control frequency (Tanaka et al., 1996). Fisher's exact test was conducted using JMP ver. 7.0.1 (SAS Institute Japan, Co., Ltd., Tokyo, Japan) to calculate the odds ratio and its 95% confidence interval (CI).

Results

Demographics, symptomatic state, coadministered drugs with carbamazepine, and *HLA-B* diplotypes of 15 patients are summarized in Table 1. However, Patient 12 was excluded from the following statistical analyses because zonisamide was a more likely causative drug. Involvement of carbamazepine in the onset of SJS/TEN could not be excluded for the remaining 11 definite SJS/TEN patients and three probable SJS patients.

In contrast to data on Han Chinese (Chung et al., 2004) and Thai populations (Locharernkul et al., 2008), *HLA-B*1502* was not detected in this work. However, two patients with definite SJS/TEN and two patients with probable SJS carried *HLA-B*1511*. The allele frequencies of *HLA-B*1511* in the SJS/TEN groups were compared with the allele frequency in a Japanese population reported by Tanaka et al. (1996) (n = 493) instead of that in carbamazepine-tolerant patients, because the incidence of SJS/TEN in Japan is very low (three per million/year). Allele frequencies of *HLA-B*1511* increased significantly in the SJS/TEN group regardless of the exclusion or inclusion of probable SJS patients [0.0909 (2 of 22) and 0.143 (4 of 28), respectively) than in the Japanese population (0.01), and the odds ratios were 9.76 (p = 0.0263, CI 2.01–47.5) and 16.3 (p = 0.0004, CI 4.76–55.6), respectively. No patients with *HLA-B*1511* had severe ocular complications.

Discussion

Recently, *HLA-B*1502* involvement has been reported in carbamazepine-induced SJS/TEN in Southern Asian patients (Chung et al., 2004; Man et al., 2007; Locharernkul et al., 2008; Mehta et al., 2009) and patients of Asian ancestry living in Europe (Lonjou et al., 2006). Although we did not detect SJS/TEN patients receiving carbamazepine who carried *HLA-B*1502*, we did find four patients carrying *HLA-B*1511*. *HLA-B*1511* and *HLA-B*1502* belong to the same HLA-B75 serotype. Other major members of HLA-B75 are *HLA-B*1508*, *HLA-B*1515*, and *HLA-B*1521*. Mehta et al. (2009) have investigated the association between *HLA-B*1502* and carbamazepine-induced SJS using eight Indian patients. Although in their study most patients (six of eight) did carry *HLA-B*1502*, one patient was homozygous *HLA-B*1508*. Tassaneeyakul et al. (2010)have also performed a case–control study using 42 CBZ-induced SJS/TEN patients and 42 carbamazepine-tolerant controls in a Thai population. In their study, 37 SJS/TEN patients carried *HLA-B*1502* and the very strong association of *HLA-B*1502* with SJS/TEN was again confirmed. Although the statistical significance was not examined, two patients carrying heterozygous *HLA-B*1521* and one patient carrying heterozygous *HLA-B*1511* were detected, suggesting that not only *HLA-B*1502* but also some subfamilies of serotype HLA-B75 are involved in the onset of carbamazepine-induced SJS/TEN.

Allele frequencies of individual HLA genotypes in worldwide populations obtained from various studies are shown at Allelefrequencies.net (Middleton et al., 2003). Table 2 summarizes the population allele frequencies of representative types of HLA-B75 in various ethnic groups. In Han Chinese, Thai and Indians, carriers of *HLA-B*1502*, *HLA-B*1521*, and *HLA-B*1508* are at high risk of carbamazepine-induced SJS/TEN, although *HLA-B*1502* is mainly involved. A comparable allele frequency of *HLA-B*1511* (higher than 3.8%) to that of *HLA-B*1502* in Han Chinese in Beijing has been reported recently by Yang et al. (Yang et al., 2010). Because the allele frequency of *HLA-B*1511* is higher than that of *HLA-B*1502* in Japanese and Koreans, carriers of the former may more easily be detected in association studies than carriers of the latter in northeast Asian populations. *HLA-B*1521* can be a risk

Epilepsia, 51(12):2461–2465, 2010
doi: 10.1111/j.1528-1167.2010.02766.x

Table 1. Backgrounds and HLA-B diplotypes of Japanese carbamazepine-related SJS/TEN patients

ID[a]	ADR type	Sex/Age	Severity score in ophthalmic disorders	Highest BT (°C)	Total area of blistering skin (%)	Systemic complications	Result of DLST to CBZ	Period of onset for CBZ (days)	Coadministered drugs: Drug name	Coadministered drugs: DLST result/period of onset	HLA-B diplotype: High resolution	HLA-B diplotype: Low resolution
1 (1)	TEN	M/73	1	>39	20	Neutropenia	−	14	Potassium citrate/sodium citrate hydrate	−/4 days	**1511**/4801	**B75**/B48
						Liver dysfunction			Allopurinol	−/>5 years		
									Etizolam	−/>5 years		
									Sodium pravastatin	−/>5 years		
2 (5)[b]	SJS	F/6	At least 1[c]	>37.0	<10%	GI tract disturbance	Not tested	9	None		4006/5101	B61/B51
3 (6)[b]	SJS	F/52	At least 1[c]	Unknown	<10%	Neutropenia	Not tested	14	Zonisamide	Not tested/346 days	4601/5901	B46/B59
						Liver dysfunction						
4	SJS	M/52	0	38	1	GI tract disturbance	Not tested	51	Tegafur/gimeracil/oteracil potassium	Not tested/38 days	0702/5201	B7/B52
						Neutropenia						
						Liver dysfunction						
						Renal dysfunction						
5	SJS	M/32	1	39	5	Liver dysfunction	Not tested	42	None		4002/5401	B60/B54
6 (2)	SJS	F/42	3	>39	5	GI tract disturbance	−	Shorter than 34	Sodium diclofenac	−/1 year	4001/5201	B60/B52
									L-carbocysteine	−/1 year		
									Cefteram pivoxil	−/4 days		
									Olopatadine hydrochloride	Not tested/unknown		
7	SJS	F/64	At least 1[c]	>37.0	10	Liver dysfunction	+	13	Mecobalamin	Not tested/13 days	**1511**/4002	**B75**/B60
8 (3)	SJS	M/45	3	>37.0	5	Liver dysfunction	Not tested	49	None		4801/5601	B48/B56
9 (4)	SJS	M/54	0	<37.0	0.5	None	+	34	None		1501/3501	B62/B35
10	TEN	M/38	3	40.3	40	Liver dysfunction	+	15	Troxipide	−/8 days	1302/4403	B13/B44
									Levofloxacin hydrate	−/15 days		
									Mecobalamin	−/9 days		
									Acyclovir	−/9 days		
11 (7)	TEN	M/17	3	39.7	20	Respiratory involvement	+	5	Zonisamide	+/33 days	4601/5601	B46/B56
						Neutropenia			Amoxicillin hydrate	+/1 day		
						Liver dysfunction			Promethazine methylenedisalicylate	Not tested/1 day		
12[d]	SJS	M/6	1	Unknown	<10%	Liver dysfunction	−	145	Zonisamide	+/24 days	**1511**/4006	**B75**/B61
13	Probable SJS	F/54	Unknown	<37.0	>10%	Liver dysfunction	Not tested	22	Sodium pravastatin	Not tested/unknown	4006/4403	B61/B44
									Nifedipine	Not tested/81 days		
									Etizolam	Not tested/15 days		
									Lansoprazole	Not tested/46 days		
									Sodium risedronate hydrate	Not tested/46 days		
14	Probable SJS	F/36	At least 1[c]	Unknown	5	None	+	15	Timiperone	Not tested/1 day	1301/**1511**	B13/**B75**
15	Atypical SJS	F/65	1	37.4	0.1	None	+	9	None		**1511**/3501	**B75**/B35

BT, body temperature; DLST, drug lymphocyte stimulation test; CBZ, carbamazepine.
[a]Number in parentheses is ID # from our previous study (Kaniwa et al., 2008).
[b]These patients were also included in Ikeda et al. (2010)
[c]Ophthalmic complications were observed, but severity was unknown.
[d]This patient was excluded from statistical analyses due to likely zonisamide-induced SJS.

Epilepsia, 51(12):2461–2465, 2010
doi: 10.1111/j.1528-1167.2010.02766.x

Table 2. Population allele frequencies of individual types of HLA-B75 in various ethnic groups

Ethnic group	Population allele frequencies reported in allelefrequencies.net website[a]				
	*HLA-B*1502*	*HLA-B*1515*	*HLA-B*1521*	*HLA-B*1508*	*HLA-B*1511*
Japanese	0.001	Data unavailable	Data unavailable	Data unavailable	**0.004–0.008**[b,c]
Koreans	0.002	0.000	0.000	0.000	0.020
Han Chinese	**0.019–0.124**[b]	0.010	0.000–0.002	0.005–0.015	0.000–0.017[d]
Thai	**0.061–0.085**[b]	Data unavailable	**0.007–0.010**[b]	0.010	**0.010**[b]
Indians	**0.000–0.060**[b]	Data unavailable	Data unavailable	**0.005–0.033**[b]	Data unavailable
Caucasians (West Europe)	0.000	0.000	0.000	0.000–0.004	0.000–0.003
Caucasians (East Europe)	0.000	0.000	0.000	0.000–0.009	0.000
Sub-Saharan Africans	0.000	0.000–0.008	Data unavailable	0.000	0.000
Hispanics	0.000	0.004–0.008	0.000	0.000–0.006	0.000
Arabians	0.000	0.000	0.000	0.000–0.007	0.000
Australian aborigine	0.000–0.007	Data unavailable	0.026–0.135	Data unavailable	Data unavailable

[a]New Allele Frequency Database: http://www.allelefrequencies.net/ (Middleton et al., 2003).
[b]SJS/TEN patients carrying the allele shown in the second row have been reported in the study using an ethnic group shown in the first column.
[c]The frequency of 0.1 was reported by Tanaka et al. (1996).
[d]Higher value than 0.038 in Han Chinese in Beijing was recently reported by Yang et al. (2010).

factor for carbamazepine-induced SJS/TEN for Thai and Australian aborigine. Interestingly, HLA-B75 has not been detected in carbamazepine-induced SJS/TEN Caucasian patients (Lonjou et al., 2006). This may be due to extremely low allele frequencies or no existence of HLA-B75 subfamilies.

*HLA-B*1502* has been reported to have associations with SJS/TEN caused by other aromatic antiepileptic drugs such as phenytoin and lamotrigine in Han Chinese and Thai (Man et al., 2007; Locharernkul et al., 2008). In this study we detected a patient carrying *HLA-B*1511* whose causative drug was probably zonisamide, an aromatic antiepileptic drug. Therefore, *HLA-B*1511* may be also involved in the onset of SJS/TEN induced by other aromatic antiepileptic drugs as well as *HLA-B*1502*, although further investigation is needed.

The odds ratio of *HLA-B*1511* for SJS/TEN obtained in this study was low in comparison with those observed in Thai, Indians, and Han Chinese in Taiwan (25.5, 71.4, and 25.04 respectively) (Chung et al., 2004; Locharernkul et al., 2008; Mehta et al., 2009). One reason for this may be the low allele frequency (<0.01) of *HLA-B*1511* among the Japanese. The administration of multiple drugs to Japanese patients may also contribute to the low odds ratio. Indeed, on average, more than three drugs were administered to the patients in this study. We concluded that patients receiving multiple drugs developed SJS/TEN due to carbamazepine by comparing the periods of latency of the individual drugs prior to SJS/TEN onset. However, we cannot completely exclude the possibility of other causative drugs. Another possibility is that *HLA-B*1502* is more prone than *HLA-B*1511* to cause carbamazepine-induced SJS/TEN. Carbamazepine or its metabolites may covalently (Weltzien et al., 1996) or noncovalently (Wu et al., 2007; Yang et al., 2007) bind more easily to the HLA-B*1502 protein or its binding peptide.

There are no SJS/TEN patients carrying *HLA-B*1511* who had severe ocular complications. This result coincides with the previous report that none of the 71 SJS/TEN patients with ocular surface complications had *HLA-B*1511* (Ueta et al., 2008).

Acknowledgments

This study was supported in part by the Health and Labor Sciences Research Grant (Research on Advanced Medical Technology) from the Ministry of Health, Labor and Welfare. We deeply appreciate the Federation of Pharmaceutical Manufacturers' Association of Japan for their assistance in recruiting patients. We also thank all patients and medical doctors for their cooperation with our study. We thank Ms. Sachiko Tsutsumi, Ms. Hina Kato, Dr. Akiko Miyamoto, and Mr. Jun Nishikawa for their assistance.

Disclosure

We confirm that we have read the Journal's position on issues involved in ethical publication and affirm that this report is consistent with those guidelines. None of the authors has any conflict of interest to disclose.

References

Bastuji-Garin S, Rzany B, Stern RS, Shear NH, Naldi L, Roujeau JC. (1993) Clinical classification of cases of toxic epidermal necrolysis, Stevens–Johnson syndrome, and erythema multiforme. *Arch Dermatol* 129:92–96. The diagnostic criteria are reflected in the currently used following Japanese guidance; Diagnostic criteria of Stevens–Johnson syndrome (Hashimoto K representing a Research Group on the Conquest of Intractable Diseases, Health and Labor Sciences Research Grant from the Ministry of Health, Labor and Welfare, 2005) and Diagnostic criteria of Toxic Epidermal Necrolysis (Hashimoto K representing a Research Group on the Conquest of Intractable Diseases, Health and Labor Sciences Research Grant from the Ministry of Health, Labor and Welfare, 2005).

Chung WH, Hung SI, Hong HS, Hsih MS, Yang LC, Ho HC, Wu JY, Chen YT. (2004) Medical genetics: a marker for Stevens–Johnson syndrome. *Nature* 428:486.

Ikeda H, Takahashi Y, Yamazaki E, Fujiwara T, Kaniwa N, Saito Y, Aihara M, Kashiwagi M, Muramatsu M. (2010) HLA Class I markers in

Japanese patients with carbamazepine-induced cutaneous adverse reactions. *Eplepsia* 51:297–300.

Kaniwa N, Saito Y, Aihara M, Matsunaga K, Tohkin M, Kurose K, Sawada J, Furuya H, Takahashi Y, Muramatsu M, Kinoshita S, Abe M, Ikeda H, Kashiwagi M, Song Y, Ueta M, Sotozono C, Ikezawa Z, Hasegawa R; JSAR research group. (2008) HLA-B locus in Japanese patients with anti-epileptics and allopurinol-related Stevens–Johnson syndrome and toxic epidermal necrolysis. *Pharmacogenomics* 9:1617–1622.

Locharernkul C, Loplumlert J, Limotai C, Korkij W, Desudchit T, Tongkobpetch S, Kangwanshiratada O, Hirankarn N, Suphapeetiporn K, Shotelersuk V. (2008) Carbamazepine and phenytoin induced Stevens–Johnson syndrome is associated with HLA-B*1502 allele in Thai population. *Epilepsia* 49:2087–2091.

Lonjou C, Thomas L, Borot N, Ledger N, de Toma C, LeLouet H, Graf E, Schumacher M, Hovnanian A, Mockenhaupt M, Roujeau JC; RegiSCAR Group. (2006) A European study of HLA-B in Stevens–Johnson syndrome and toxic epidermal necrolysis related to five high-risk drugs. *Pharmacogenet Genomics* 18:99–107.

Man CB, Kwan P, Baum L, Yu E, Lau KM, Cheng AS, Ng MH. (2007) Association between HLA-B*1502 allele and antiepileptic drug-induced cutaneous reactions in Han Chinese. *Epilepsia* 48:1015–1018.

Mehta TY, Prajapati LM, Mittal B, Joshi CG, Sheth JJ, Patel DB, Dave DM, Goyal RK. (2009) Association of HLA-B*1502 allele and carbamazepine-induced Stevens–Johnson syndrome among Indians. *Indian J Dermatol Venereol Leprol* 75:579–582.

Middleton D, Menchaca L, Rood H, Komerofsky R. (2003) Brief communication. New allele frequency database: http://www.allelefrequencies.net. *Tissue Antigens* 61:403–407.

Tanaka H, Akaza T, Juji T. (1996) Report of the Japanese central bone marrow data center. *Clin Transpl* 1996:139–144.

Tassaneeyakul W, Tiamkao S, Jantararoungtong T, Chen P, Lin SY, Chen WH, Konyoung P, Khunarkornsiri U, Auvichayapat N, Pavakul K, Kulkantrakorn K, Choonhakarn C, Phonhiamhan S, Piyatrakul N, Aungaree T, Pongpakdee S, Yodnopaglaw P. (2010) Association between HLA-B*1502 and carbamazepine-induced severe cutaneous adverse drug reactions in a Thai population. *Epilepsia* 51:926–930.

Ueta M, Sotozono C, Inatomi T, Kojima K, Hamuro J, Kinoshita S. (2008) HLA class I and II gene polymorphisms in Stevens–Johnson syndrome with ocular complications in Japanese. *Mol Vis* 14:550–555.

Weltzien HU, Moulton C, Martin S, Padovan E, Hartmann U, Kohler J. (1996) T cell immune responses to haptens. Structural models for allergic and autoimmune reactions. *Toxicology* 107:141–151.

Wu Y, Farrell J, Pirmohamed M, Park BK, Naisbitt DJ. (2007) Generation and characterization of antigen-specific CD4 + , CD8 + , and CD4 + CD8 + T-cell clones from patients with carbamazepine hypersensitivity. *J Allergy Clin Immunol* 119:973–981.

Yang CW, Hung SI, Juo CG, Lin YP, Fang WH, Lu IH, Chen ST, Chen YT. (2007) HLA-B*1502-bound peptides: implications for the pathogenesis of carbamazepine-induced Stevens–Johnson syndrome. *J Allergy Clin Immunol* 120:870–877.

Yang G, Deng YJ, Qin H, Zhu BF, Chen F, Shen CM, Sun ZM, Chen LP, Wu J, Mu HF, Lucas R. (2010) HLA-B*15 subtypes distribution in Han population in Beijing, China, as compared with those of other populations. *Int J Immunogenet* 37:205–212.

Epilepsia, 51(12):2461–2465, 2010
doi: 10.1111/j.1528-1167.2010.02766.x

J Pharmacokinet Pharmacodyn (2010) 37:575–590
DOI 10.1007/s10928-010-9176-y

Application of physiologically based pharmacokinetic modeling and clearance concept to drugs showing transporter-mediated distribution and clearance in humans

Takao Watanabe · Hiroyuki Kusuhara · Yuichi Sugiyama

Received: 6 May 2010 / Accepted: 25 October 2010 / Published online: 10 November 2010

Abstract This review illustrates the concept of a rate-determining process in the overall hepatic elimination of anionic drugs that involves transporters in the uptake process. A kinetic study in rats has demonstrated that uptake is the rate-determining process for most anionic drugs, and this is likely to hold true for the hepatic elimination of statins in humans. To simulate the effects of variations in the transporter activities on systemic and liver exposure, a physiologically based pharmacokinetic model was constructed for pravastatin, the overall elimination of which involves OATP1B1 and MRP2 in the hepatic uptake and canalicular efflux, respectively. The plasma concentrations of pravastatin in humans were successfully reproduced using the kinetic parameters extrapolated from in vitro data obtained using human hepatocytes and canalicular membrane vesicles and the scaling factors determined in rats. Sensitivity analyses showed that a variation in hepatic uptake altered the plasma concentration of pravastatin markedly, but had a small effect on the liver concentration, and vice versa for the canalicular efflux. Therefore, variation in the OATP1B1 activities will have small and large impacts on the therapeutic efficacy and adverse effect (myopathy) of pravastatin, respectively, whereas that affecting the MRP2 activities may have an opposite effect (i.e., large and small impacts on the therapeutic efficacy and side effect). This pharmacokinetic characteristics likely hold true for other anionic statins, i.e., variation of OATP1B1 is associated with the risk of adverse reactions, whereas that of sequestration mechanisms causes the variation of their pharmacological effect.

This manuscript is from the symposium on the occasion of Professor Malcolm Rowland's 70th birthday

T. Watanabe · H. Kusuhara · Y. Sugiyama (✉)
Laboratory of Molecular Pharmacokinetics, Graduate School of Pharmaceutical Sciences,
The University of Tokyo, 7-3-1 Hongo, Bunkyo-ku, Tokyo 113-0033, Japan
e-mail: sugiyama@mol.f.u-tokyo.ac.jp

Keywords In vitro–in vivo extrapolation · Physiologically-based pharmacokinetic model · Rate-determining process · Transporter · Uptake

Introduction

Cumulative studies have demonstrated the importance of drug transporters in drug absorption, distribution and elimination [1–7]. The liver is the major clearance organ for drugs in the body where drugs are removed from the blood circulation by metabolism and biliary excretion. Hepatocytes, the parenchyma cells of the liver accounting for 80% of the liver volume, are responsible for the hepatic metabolism and biliary excretion of drugs. Hepatocytes are characterized by distinct and functionally different plasma membranes, sinusoidal and canalicular membranes where solute carrier (SLC)-type and ATP–binding cassette (ABC)-type transporters are expressed (Fig. 1). These transporters are responsible for directional transport of drugs across hepatocytes from the circulating blood to the bile [8, 9]. Moreover, the substrates of uptake transporters include those of metabolizing enzymes. For instance, atorvastatin, cerivastatin and repaglinide are taken up by OATP1B1 followed by metabolism by cytochrome P450s (CYPs) such as CYP3A4 and CYP2C8 [10–15].

The clearance concept has been widely used for the analysis and prediction of pharmacokinetics of drugs [16–20]. A physiologically-based pharmacokinetic (PBPK) model has been used to predict the time-profiles of plasma and tissue

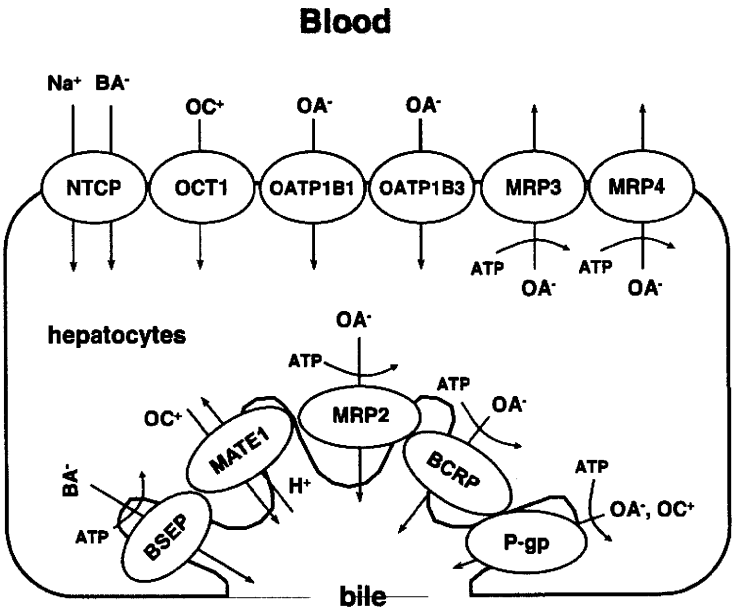

Fig. 1 Transporters acting in the hepatobiliary disposition of drugs in human. *BSEP* bile salt export pump, *MATE* multidrug and toxin extrusion protein, *MRP* multidrug resistance associated protein, *BCRP* breast cancer resistant protein, *P-gp* P-glycoprotein, *NTCP* sodium-taurocholate cotransporting polypeptide, *OCT* organic cation transporter, *OATP* organic anion transporting polypeptide, *OAT* organic anion transporter, *BA* bile acids, OA^- organic anion, OC^+ organic cation

concentrations of drugs [21, 22]. The PBPK model is useful for simulating the disposition of drugs in the body using drug-dependent kinetic parameters as well as physiological parameters. It is also helpful to examine the effects of variations in physiological and kinetic parameters, which are caused by a disease state, drug–drug interactions (DDI) and genetic variations, on the exposure of drugs in the blood and organs and, ultimately, their effects on the pharmacological and/or toxicological actions of drugs [15, 23].

In this review article, we would like to introduce our recent research on the in vitro-in vivo extrapolation (IVIVE) of transporter-mediated membrane transport to investigate the rate-determining process in the overall hepatic elimination, and a PBPK model including transporter-mediated transport processes to simulate the systemic and liver exposure of a model drug, pravastatin, for which transporters are deeply involved in its hepatobiliary transport in humans [9, 24, 25]. Finally, we have demonstrated the effects of variations in transporter activities, caused by genetic polymorphisms or DDIs, on the concentration profiles of pravastatin in the plasma and liver (target organ), which are closely related to the adverse reactions and pharmacological effects of the drug, respectively.

Hepatic intrinsic clearance involving membrane transport

Variation of hepatic uptake of anionic drugs

OATP1B1 and OATP1B3 play major roles in the hepatic uptake of anionic drugs [4]. This has been supported by clinical evidence, DDI and pharmacogenomic studies. The plasma AUC of cerivastatin was increased fourfold by the coadministration of cyclosporine A (CysA) [26]. We suggested that the inhibition of OATP1B1 by CysA is the underlying mechanism [12]. The uptake of cerivastatin by cryopreserved human hepatocytes was saturable, and CysA inhibited the saturable uptake of cerivastatin with a Ki value of 0.3–0.7 μM which was similar to the Ki value (0.2 μM) for the uptake of cerivastatin in MDCKII cells expressing human OATP1B1. On the other hand, the Ki value of CysA for inhibition of cerivastatin metabolism in human liver microsomes was far greater than that for the uptake process (>30 μM). The unbound plasma concentration of CysA in the systemic circulation achievable by clinical dose was at most 0.1 μM, which is not enough to inhibit hepatic uptake of cerivastatin (30% inhibition) to account for the clinical data. Since CysA was given orally, it is possible that the unbound concentration in the portal vein is greater than the maximum concentration in the systemic circulation, producing more potent inhibition of OATP1B1. Recently, it has also been reported that the coadministration of rifampicin increases the plasma AUC of atorvastatin, bosentan and glibenclamide, which are substrates of both hepatic uptake transporters (OATP) and metabolic enzymes (CYP3A4 and CYP2C9) [11, 27, 28]. Rifampicin can inhibit OATP1B1 and OATP1B3 potently but not CYP3A4 and CYP2C9. The Ki values for the inhibition of OATPs are 0.5-3.2 μM, whereas those for CYPs are more than 50 μM [27, 29, 30]. The plasma concentrations of rifampicin in the clinical drug interaction study were in the range of 2.5–17 μM

following the administration of a single intravenous dose (600 mg) [11]. Taking into consideration the unbound fraction in the plasma (0.1–0.4 [31]), we calculated the unbound plasma concentration of rifampicin to range from 0.25 to 6.8 μM. These observations suggest that the DDIs were caused by the inhibition of uptake transporters by rifampicin. Although inhibition potency was lower compared with OATP1B1, it is predicted that both CysA and rifampicin are capable of inhibiting OATP1B3 at their clinical doses [30]. The in vivo relevance for this has not been reported, yet.

The effects of genetic polymorphisms in OATP1B1 on the systemic exposure of several anionic drugs have been reported by some research groups including ourselves [4, 32, 33]. Two common SNPs, A388G and T521C, have been reported. Nishizato et al. have demonstrated that the T521C mutation is linked tightly with A388G, which results in the formation of the OATP1B1*15 haplotype in Japanese and that the plasma AUC of pravastatin after oral administration in healthy subjects with the OATP1B1*15 haplotype (A388G + T521C) was significantly higher compared with that in subjects with the *1b allele (A388G) [34]. Maeda et al. have demonstrated that subjects with OATP1B1*1b have a lower plasma AUC and a higher total clearance of pravastatin and the AUC of pravastatin is well correlated with that of valsartan and temocapril, suggesting that the clearance mechanism of these three drugs may be shared mutually [35]. The functional change in the OATP1B1*15 mutant has been investigated in in vitro experiments, and three independent reports support the reduced uptake activity in the OATP1B1*15 mutant compared with wild type OATP1B1 [36–38]. Similar clinical outcomes related to *15 and T521C alleles have been reported in the case of many other drugs, such as pitavastatin, atorvastatin, rosuvastatin, valsartan, temocapril, atrasentan, irinotecan, repaglinide, nateglinide and ezetimibe [4].

Theoretical considerations

The intrinsic clearance is defined as the velocity of a metabolic or transport process divided by the drug concentration at which that process occurs. According to this definition, the overall intrinsic hepatic clearance ($CL_{int,all}$) is defined with regard to the unbound concentration of drugs in the extracellular space. As far as rapid equilibrium can be assumed, $CL_{int,all}$ is equal to the intrinsic clearance for the sequestration clearance (CL_{int}), the sum of the intrinsic clearance for metabolism and/or canalicular efflux with regard to the unbound concentration in the organ. Otherwise, $CL_{int,all}$ includes the intrinsic clearance of the uptake (PS_{inf}) and efflux (PS_{eff}) across the sinusoidal membrane (Eq. 1) (Fig. 2):

$$CL_{int,all} = PS_{inf} \cdot \frac{CL_{int}}{PS_{eff} + CL_{int}} \quad (1)$$

Equation 1 indicates three facts; (1) uptake clearance gives the maximum value of the overall intrinsic hepatic clearance, (2) CL_{int} underestimates $CL_{int,all}$ because of the concentration of unbound drug in the cytosolic compartment to the blood, and (3) the magnitude of the sequestration clearance to the sinusoidal efflux clearance, but not its absolute value, is the key factor for the overall intrinsic hepatic clearance.

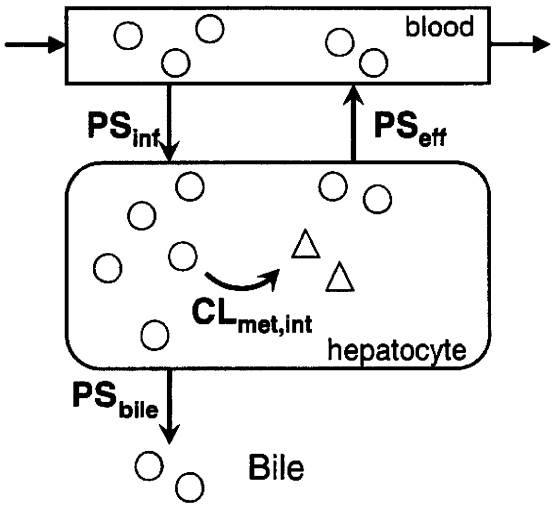

Fig. 2 Intrinsic hepatic clearance including membrane transport processes. $CL_{int,all}$, overall intrinsic hepatic clearance, PS_{inf} intrinsic uptake clearance, PS_{eff} intrinsic sinusoidal efflux clearance, PS_{bile} intrinsic biliary clearance, $CL_{met,int}$ intrinsic metabolic clearance

$$CL_{int,\,all} = PS_{inf} \cdot \frac{CL_{int}}{PS_{eff} + CL_{int}}$$

$$(CL_{int} = PS_{bile} + CL_{met,\,int})$$

It also provides a concept of a rate-determining process in the hepatic elimination. When CL_{int} is significantly greater than PS_{eff}, $CL_{int,all}$ can be approximated to PS_{inf}, and it does not depend on PS_{eff} and CL_{int}:

$$CL_{int,all} = PS_{inf} \tag{2}$$

In this case, the hepatic elimination is referred to as "uptake-limited". On the contrary, when CL_{int} is negligibly lower than PS_{eff}, $CL_{int,all}$ can be expressed as follows:

$$CL_{int,all} = PS_{inf} \times CL_{int}/PS_{eff} \tag{3}$$

In this case, all processes are related to $CL_{int,all}$. Therefore, variations in CL_{int} as well as PS_{eff} caused by DDIs or genetic polymorphisms could have an impact on the systemic exposure of drugs. Accordingly, the rate determining process must be taken into consideration to predict the impact of a variation in metabolic and/or biliary excretion activity on the systemic exposure of drugs, whereas a change in uptake activity consistently influences the systemic exposure of drugs.

Rate-determining process in the hepatic elimination of anionic drugs based on non-clinical experiments

Comparison of the tissue uptake clearance with hepatic clearance determines if the hepatic elimination is uptake-limited. Before our study, the only drug reported to show uptake-limited hepatic elimination in rats was methotrexate [39]. We investigated the rate-determining process in the overall hepatic elimination of pravastatin in rats [40]. The intrinsic biliary clearance (PS_{bile}) and the intrinsic metabolic clearance ($CL_{met,int}$) were determined by steady-state analysis, and the

intrinsic sinusoidal efflux clearance (PS_{eff}) was assumed to be identical to the passive diffusion clearance across the membrane in freshly isolated rat hepatocytes, because there is no method of directly measuring this parameter and there is no evidence that transporters are involved in the sinusoidal efflux of pravastatin in the liver. PS_{bile}, $CL_{met,int}$ and PS_{eff} were estimated to be 1.14, 1.33, and 0.192 ml/min/g liver. The sequestration clearance was 13-fold greater than PS_{eff}, indicating that hepatic uptake is the rate-determining process in the overall hepatic elimination of pravastatin. To support this, the in vivo PS_{inf} of pravastatin was determined by the multiple indicator dilution (MID) technique in rats [41]. It was comparable with the in vivo $CL_{int,all}$. In addition to pravastatin, this holds true for atorvastatin and fluvastatin, but not pitavastatin, the in vivo PS_{inf} of which was half the in vivo $CL_{int,all}$ [41]. Furthermore, Watanabe et al. determined the uptake clearance of twelve anionic drugs, the main clearance mechanism of which is biliary excretion, by integration plot analysis (Fig. 3) [42]. The uptake clearance of nine of these drugs was similar to the hepatic clearance. These data indicate that the uptake process is rate-determining in the hepatic elimination of most anionic drugs in rats. In addition, the finding that in vitro uptake clearance determined using isolated rat hepatocytes of test drugs is similar to the in vivo value except for a few drugs. This prompted us to estimate the hepatic uptake clearance of statins (pravastatin, pitavastatin, atorvastatin and fluvastatin) in humans using human cryopreserved hepatocytes. We determined the uptake clearance of the four statins using several batches of single-donor hepatocytes, which had been confirmed by prescreening to retain sufficient transport activities for the typical OATP and NTCP substrates, estradiol-17β-glucuronide and taurocholate, respectively. The estimated values are relatively comparable with the values of $CL_{int,all}$ in humans (Fig. 4), suggesting that the uptake process is rate-determining in the hepatic elimination of the four statins. It is worth mentioning that, among the four statins, the major elimination

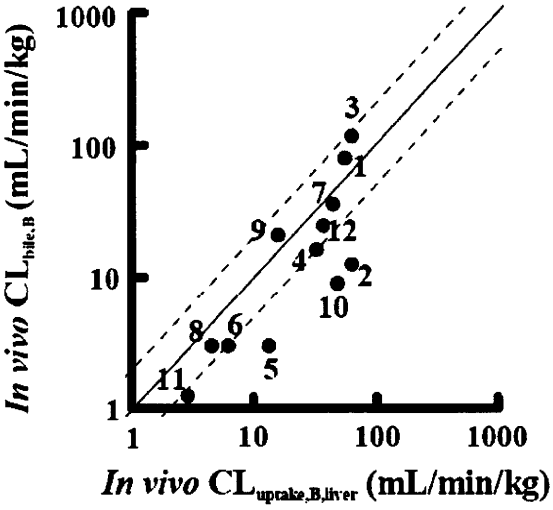

Fig. 3 Comparison between in vivo organ clearance ($CL_{bile,B}$) and organ uptake clearance ($CL_{uptake,B,liver}$) in the liver [42]. $CL_{uptake,B,liver}$ values were obtained from integration plot analyses. *Plots* represent the following: 1, pravastatin; 2, pitavastatin; 3, rosuvastatin; 4, valsartan; 5, olmesartan; 6, candesartan; 7, temocaprilat; 8, enalaprilat; 9, benazeprilat; 10, benzyl penicillin; 11, ceftizoxime; and 12, cefmetazole. The *solid line* represents the line of unity, and the *dashed lines* represent the lines of 1:2 and 2:1 correlations

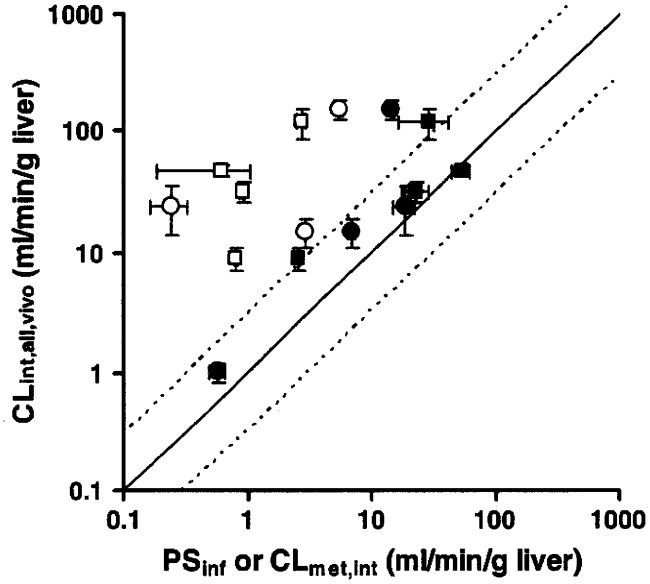

Fig. 4 Comparison of the in vivo hepatic overall intrinsic clearance of statins with the in vitro hepatic uptake clearance or metabolic clearance ([41] with modification). In vivo hepatic overall intrinsic clearances of statins in rats and humans are plotted against the in vitro uptake clearance or metabolic clearance. *Filled circle*, uptake clearance determined using human hepatocytes; *open circle* metabolic clearance determined using human liver microsomes; *filled square*, uptake clearance determined using rat hepatocytes; *open square*, metabolic clearance determined using rat liver microsomes. The *straight line* indicates a 1:1 correlation, and the *dashed lines* represent the lines of 1:3 and 3:1 correlations

mechanism of atorvastatin and fluvastatin is metabolism by CYPs [15], and the $CL_{met,int}$ determined in vitro considerably underestimated the $CL_{int,all}$ (Fig. 4). Thus, whether hepatic uptake involves a transporter or not is a critical factor in predicting hepatic intrinsic clearance from in vitro data. It is possible that this holds true for other bisubstrates of uptake transporters and metabolizing enzymes, such as cerivastatin, repaglinide, nateglinide, bosentan and telmisartan [27, 43–48], and further studies are needed. These results indicate that IVIVE for those drugs should be performed based on the in vitro uptake data as well as metabolism taking the rate-determining process into consideration.

PBPK modeling

In a PBPK model, compartments representing actual tissues are connected by blood flow to represent the disposition of drugs in the body. The major advantage of a PBPK model is that it can allow deep understanding of the factors governing the systemic exposure and tissue distribution of drugs, and simulate the impact of variations in physiological and/or drug related parameters on the disposition once it is constructed. Application of PBPK modeling is recommended for quantitative estimation of the relative importance of uptake and efflux transporters in the pharmacokinetics of drugs in vivo in humans, and also for the initial predictions of the potential of drug interactions [2]. We constructed a PBPK model including transporter-mediated membrane transport processes to predict the pharmacokinetics

of pravastatin in humans, and to obtain an insight into the effect of variations in transporter function caused by DDIs and/or genetic polymorphisms on the pharmacokinetics and the pharmacological and/or toxicological effects [40]. The hepatic uptake of pravastatin is mainly mediated by OATP1B1, and its biliary excretion is predominantly mediated by MRP2. Physiological parameters, such as tissue weight and blood flow rate, were cited from previous reports [22, 49], and in vivo intrinsic clearances of pravastatin in human were predicted by IVIVE using the in vitro parameters determined in human derived materials and the scaling factors (SFs) determined in rats [50]. The details of the IVIVE will be described in the next section.

Construction of a PBPK model

The PBPK model consists of compartments corresponding to the liver (clearance and pharmacological target organ), a rapid equilibrium compartment, and the peripheral organs, such as the muscle and kidney, to describe the disposition of pravastatin in rats and humans (Fig. 5a) [40]. The initial distribution volume, which was estimated by fitting the rat in vivo data to a two-compartment model, was used as the volume of the rapid equilibrium compartment, including the blood compartment, assuming no obvious interspecies differences [40]. The liver was divided into five units consisting of the extracellular and subcellular compartments.

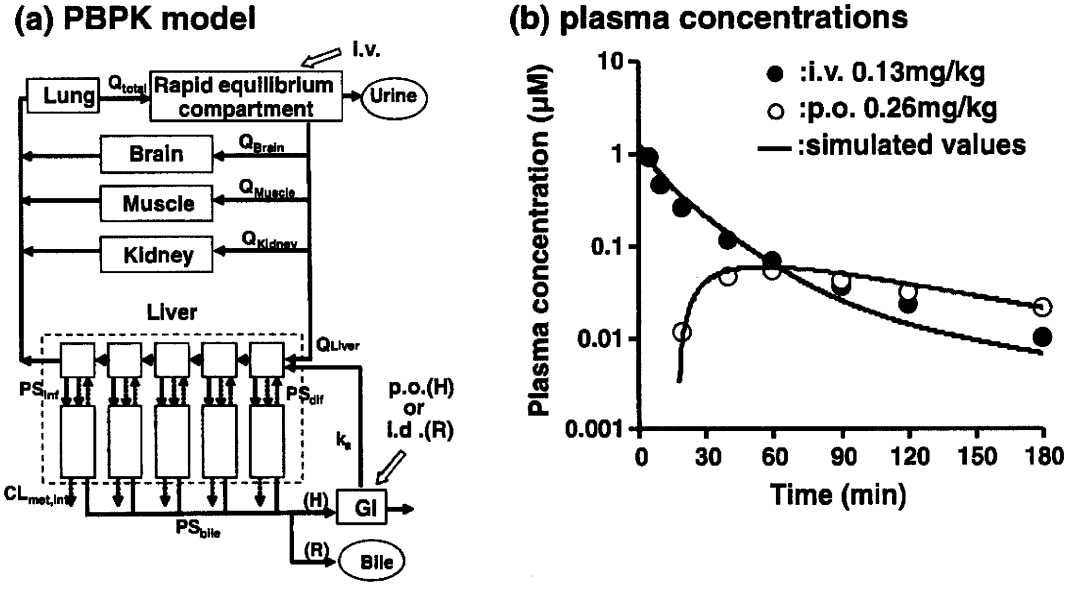

Fig. 5 Physiologically-based pharmacokinetic model, and the predicted plasma concentration–time profiles of pravastatin following intravenous and oral administration ([40] with modification). **a** The liver consists of five units connected in tandem by blood flow rate to mimic the dispersion model. The enterohepatic circulation was considered in humans given pravastatin orally (p.o.) (H), but not in rats (R) given pravastatin intraduodenally (i.d.) because bile was collected in rats. **b** The plasma concentrations were predicted using the PBPK model and kinetic parameters extrapolated from in vitro data using scaling factors determined in rats. The absorption rate constant was estimated by noncompartment analysis using the plasma concentration data, and was set at 0.0078 min^{-1}. A lag time of 17 min was taken into consideration in the simulation of oral administration. The fraction absorbed was deemed to be 0.47, which was estimated from the bioavailability (0.18) and hepatic availability (0.38) of the drug [54]

Each unit was connected in tandem by blood flow. This tank model was introduced to mimic the "dispersion" model because the hepatic elimination of pravastatin is blood-flow limited in rats, and the "dispersion" model is the appropriate model to describe the hepatic availability of such a high-clearance drug [19, 20, 50, 51]. The number of liver compartments (n in Eq. 4) was determined to be minimum integer giving the F_h value closest to the hepatic availability calculated based on the assumption of the dispersion model. The hepatic availability (F_h) following the tank model is expressed as follows;

$$F_h = \left(Q_h/\left(Q_h + f_B\left(CL_{int,all}/n\right)\right)\right)^n \quad (4)$$

where Q_h represents the hepatic blood-flow rate. Using the kinetic parameters related to hepatic clearance, such as PS_{inf}, PS_{dif}, PS_{bile}, and $CL_{met,int}$, determined by in vivo experiments, and the other drug-related and physiological parameters in rats, the concentrations in the plasma and liver, and biliary excretion-time profiles for pravastatin were successfully reproduced under both linear and nonlinear conditions. The SFs for the hepatic uptake and canalicular efflux of pravastatin were determined to be 3.7 and 21, respectively, by dividing the in vivo values by the corresponding in vitro parameters in rats. To predict the in vivo hepatic uptake and canalicular efflux clearances of pravastatin in humans, the in vitro parameters determined in human cryopreserved hepatocytes and canalicular membrane vesicles were multiplied by the rat SFs, assuming that there is no significant interspecies difference in the SFs. In vitro saturable and nonsaturable uptake clearances by the hepatocytes were obtained from full kinetic analyses in rats, and simply by the use of low and high substrate concentrations in humans. The ATP-dependent uptake clearance at trace concentration in rat and human canalicular membrane vesicles, which was calculated by subtracting the uptake in the absence of ATP from that in the presence of ATP, was used as the in vitro biliary clearance, PS_{bile}. The clearance of the nonsaturable component with regard to the unbound concentration in the liver was determined in vivo in rats. The same parameter was used in the simulation of pravastatin disposition in humans, assuming negligible species differences in this parameter between rats and humans. Simulated plasma concentration–time profiles of pravastatin after intravenous and oral administration were fairly close to the observed values in humans (Fig. 5b), showing that the predicted values were not far from the true values.

Sensitivity analysis: relationship between transporter activity and pharmacological/toxicological action of pravastatin

For pravastatin, hepatic exposure is critical for its pharmacological effect. Based on the pharmacokinetic concepts, the AUC of liver (AUC_h) can be expressed by Eq. 5 [40]:

$$\frac{Dose}{f_h \cdot AUC_h} = CL_{int} + \frac{Q_h \cdot CL_r}{CL_r + Q_h} \frac{PS_{eff} + CL_{int}}{f_b \cdot PS_{inf}} \quad (5)$$

where Q_h and CL_r represent the hepatic blood flow rate and the renal clearance, respectively, and f_b and f_h are the unbound fractions in the blood and liver,

respectively. PS_{inf}, PS_{eff} and CL_{int} are the hepatic uptake, sinusoidal efflux and intrinsic sequestration clearance, respectively. When CL_r is negligible, Eq. 5 can be simplified to:

$$\frac{Dose}{f_h \cdot AUC_h} = CL_{int} \tag{6}$$

Equation 6 suggests that the AUC_h is governed only by the sequestration clearance from the liver, but not by either uptake or sinusoidal efflux clearances. Namely, rather than the uptake process, changes in metabolic clearance and/or biliary clearance greatly affect the pharmacological action of statins as far as the renal elimination is negligible.

To show the effect of variations in pharmacokinetic parameters on the plasma and liver concentrations of pravastatin, sensitivity analysis was performed. Plasma and liver concentrations after oral administration (40 mg) were simulated using the PBPK model with varying hepatic transport activities, canalicular efflux or sinusoidal efflux over a 1/3- to threefold range of the initial values (Fig. 6) [40]. Changes in hepatic uptake markedly altered plasma pravastatin concentrations, with small effects on liver concentrations, and vice versa for the canalicular efflux. These are in a good agreement with the kinetic considerations. It is worth noting that the impact caused by variation of PS_{inf} on the plasma AUC was greater than that predicted based on the well-stirred model. The simulation showed that the plasma AUC was reduced to 14% of the initial value when PS_{inf} becomes three times greater, whereas the well-stirred model predicts that it should be reduced to 33%. Figure 7 provides a clue to understand the reason of this discrepancy. It shows the relationship between PS_{inf} and the plasma AUC after the oral administration of the drug (40 mg), calculated from the hepatic availability and total-body clearance, based on the well-stirred, parallel tube, and dispersion models [16–20], in which PS_{inf} was included in $CL_{int,all}$ (Eq. 1). Particularly, for high extraction drugs, the well-stirred model underestimates the hepatic clearance compared with the parallel tube and dispersion models, and the difference becomes greater along with an increase in PS_{inf} irrespective of the contribution of renal elimination (Fig. 7a, b). This is the case for pravastatin, for which the hepatic availability is 0.38, when the model dependence on the hepatic availability is minimal. However, when PS_{inf} increases threefold, the availability of pravastatin in the liver shows a clear dependence on the model.

As described in "Variation of hepatic uptake of anionic drugs" section, clinical studies have demonstrated that the genetic variations of OATP1B1 and DDIs involving OATP1B1 are associated with interindividual differences in the systemic exposure of pravastatin and other substrate drugs. It is reasonable that the frequency of the OATP1B1*15 haplotype was significantly higher in patients who experienced myopathy after receiving pravastatin or atorvastatin than in patients without myopathy [52], and that the variants in OATP1B1 are strongly associated with an increased risk of simvastatin-induced myopathy [53] because of higher exposure to the muscle. The simulation suggests that liver concentrations of pravastatin are slightly affected by an alteration of the uptake activity. This is because renal elimination makes a significant contribution to the systemic elimination of